Using the CQUAD4 Element to Model the Interface Between Solid and Shell Finite Elements

David S. Mc Collum

Micro Motion, Inc.
7070 Winchester Circle
Boulder, Colorado 80301

Abstract

The MSC/NASTRAN **CQUAD4** shell element is used to facilitate the transition modelling at the interface between shell and solid elements. The **CQUAD4** element is used in lieu of multi-point constraints or rigid elements. By "coating" the solid surface at the *plane* defining the transition interface, degree-of-freedom consistency is maintained. The element thickness t and the normalized bending inertia $12I/t^3$ are also varied in order to study their effects on the transition modelling. The impetus for using the **CQUAD4** element arises from its ease of application at an interface, particularly when a graphics pre/post-processing program is used to construct the finite element model and when the model geometry is complex. The efficacy of using the **CQUAD4** at a shell/solid transition interface is investigated for typical analysis problems.

1 Introduction

Many finite element models contain regions where either shell or solid finite elements are more appropriately implemented. Typically, solid finite elements are preferred in regions where complex, three-dimensional stress states occur. However, many regions are modelled quite well, and more efficiently, by shell elements. The difficulty in finite element modelling occurs at the point where solid and shell elements are connected. At these points, a discrepancy in the transfer of some degrees-of-freedom (*dof*) between the different types of elements exists. Since solid elements do not possess rotational *dof*, some technique must be used to account for the in-plane rotational *dof* of the shell elements. The goal of the finite element analyst is to create the simplest model without sacrificing accuracy. It is important to have a good transmission of mechanical behavior through the interface between solid and shell finite elements. Modelling the mesh interface well is necessary in order to minimize any possible adverse effects associated with the transition from solid to shell elements.

Three important aspects of the interface must be considered, namely, kinematic compatibility, care taken not to over-constrain motion at the interface, and the simplicity of application of the particular chosen technique[1]. If the interface is incorrectly modelled, forces, moments, and displacements may not be properly transmitted through the interface. Also, stress perturbations may occur across the interface.

The conventional wisdom for modelling the mesh interface suggests the utilization of *multi-point constraints*, so-called *rigid elements*, and *interpolation constraint elements*. Of the "element" variety, the MSC/NASTRAN **RBAR** and **RBE3** elements are quite good[1]. For larger problems especially,it may be quite laborious to implement these techniques, even using a graphics pre/post-processing program.

As an alternative to the above conventional techniques, the MSC/NASTRAN **CQUAD4** shell finite element is used herein to model the mesh interface[2]. At an interface, the face of the solid element is usually perpendicular to the plane of the shell element. Without additional modelling, the two, *in-plane* rotations of the shell element have no connection to the solid element. By "coating" the surface of the face of the solid element at the interface, one of the two rotational *dof* is accounted for. The remaining rotational *dof* of the interface shell element and the regular shell element remain free. In this case, a displacement discontinuity along their common edges could result.

Normally, it is not recommended to model a curved surface with **CQUAD4** elements where the angle between the planes of any two adjoining elements is greater than 10°. Since each node has five *dof*, the larger the angle between adjoining elements, the greater the kinematic incompatibility[3, pp. 235–245]. Figure 1 shows the intersection between two shell elements. The incompatible rotational *dof* are shown by gray arrows. The translational *dof* in Figure 1 are shown by single-headed arrows and

Figure 1: Kinematic *dof* at the intersection between two CQUAD4 elements.

the rotational *dof* by double-headed arrows. The incompatible *dof* are the in-plane bending rotations perpendicular to the edges of intersection. Although a kinematic incompatibility is created when the CQUAD4 elements meet at angles considerably away from a planar intersection, e.g. at 90° in this study, mechanical behavior is not drastically effected. In most models, it is an easy task to select the faces of the solid elements at the interface and to generate the shell (CQUAD4) elements as a surface coating. This is greatly facilitated when the analyst uses a graphical pre/post-processor. This is the main impetus for using the CQUAD4 element at the interface between solid and shell elements.

An essential aspect of the implementation of the CQUAD4 element is the specification of the thickness t and the normalized bending inertia $12I/t^3$ for the interface shell elements. Herein, the CQUAD4 shell elements used at the interface between the solid and shell elements will be referred to as the "interface elements" and the normalized bending inertia field of the MSC/NASTRAN PSHELL entry, as defined above, will be referred to as the "bending stiffness" $\mathcal{B}$ of the interface elements[4]. By *adjusting* these two parameters for the interface elements, good transmission of mechanical behavior through the interface can be achieved.

This discussion does not include extensive tests on widely varying models, nor dynamics applications, nor a sensitivity analysis of different interface techniques. In addition, a comparison between different methods of interface modelling is not presented.

It should be noted that the CQUAD4 element was chosen for application at the interface instead of, say, the MSC/NASTRAN CQUADR element due to its popularity and maturity. Of course, if the CQUADR element was used at the interface, a spurious *dof* would still exist unless the region modelled by shell elements contained CQUADR elements.

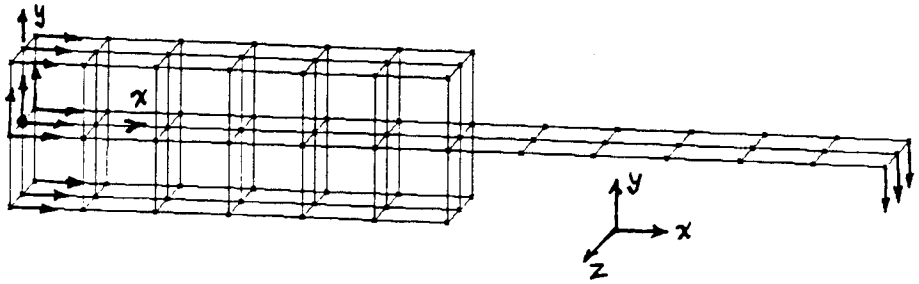

Figure 2: Case 1. The cantilevered beam model.

2 Interface Models

In this study, two simple models will be used to determine the viability of using the CQUAD4 element at an interface. The first case is a cantilevered beam under a transverse load at the free end. The second case is a cantilevered tube-beam under pressure and transverse end loads. In both cases, the solid regions are modelled by CHEXA8 elements and CQUAD4 elements are used in the shell regions.

For both analysis problems described herein, steel having a Poisson's ratio $\nu = 0.3$ and a Young's modulus $E = 30E6$ *psi*, is used.

2.1 The Cantilevered Beam Problem

The finite element model used in this case consists of a cantilevered beam structure with dimensions $6 \times 1 \times 1$ inches (See Figure 2). The solid and shell regions are each 3 inches in length. The cross-sectional area of the model is 1 in^2. The thickness of the shell region matches that of the solid region. Four interface elements are used in this model (See Figure 3). A load of 150 *lb.* is applied to the free end of the beam.

The goal in this case is to determine whether or not a set of parameters, i.e., the interface shell thickness t_i and bending stiffness $\mathcal{B}$, can produce the desired force/moment transmission through the interface. In the analysis, t_i was assigned values of 1.0, 0.1, and 0.01, while $\mathcal{B}$ was assigned values of 1, 10, 100, 1,000, 10,000, and 100,000. Permuting the values for the parameter set $\{t_i, \mathcal{B}\}$ yielded eighteen subcases.

An inadequate set of values of the parameters $\{t_i, \mathcal{B}\}$ produces the effect shown in Figure 4. When an appropriate set of values is used, the proper bending action of the entire beam model is realized (See Figure 5).

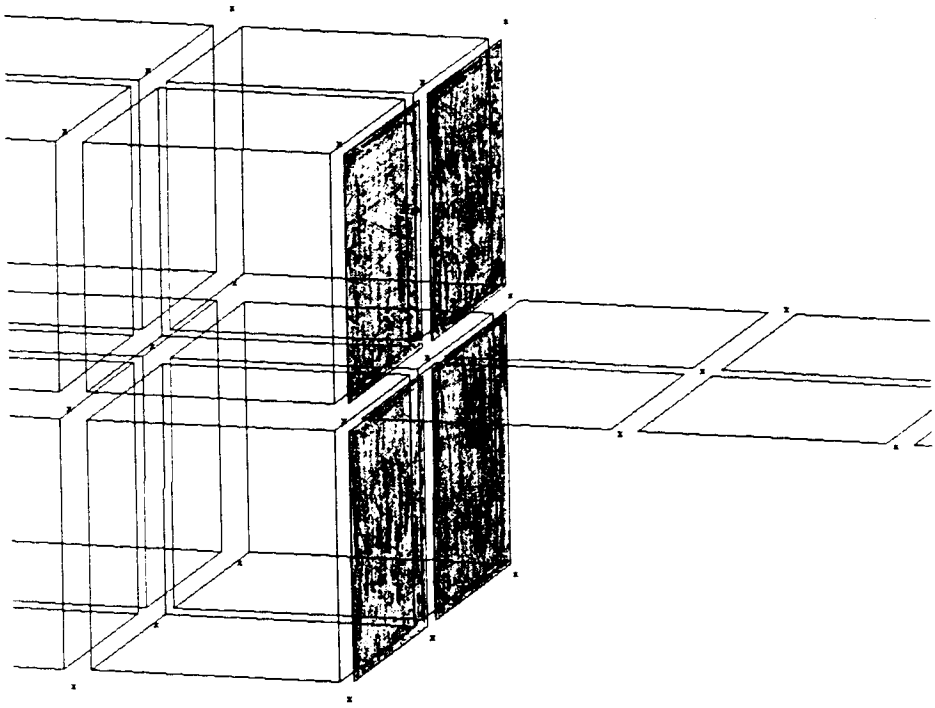

Figure 3: Case 1. Detail of the beam model solid/shell interface.

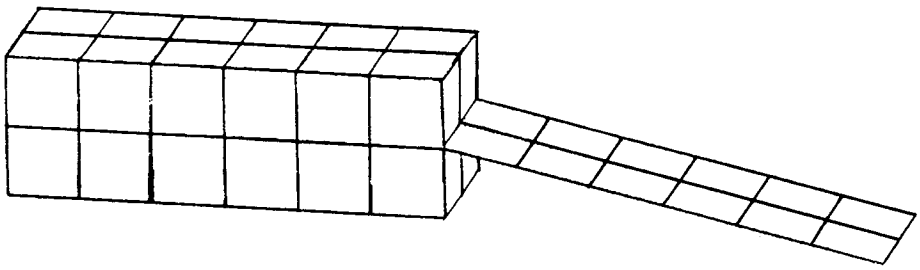

Figure 4: "Hinging" displacement behavior due to the insufficient bending stiffness of the interface elements.

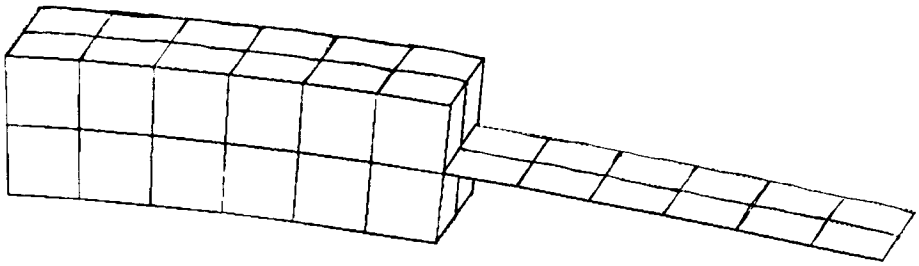

Figure 5: Proper bending behavior of the cantilevered beam model.

Analysis Results

The displacement of the beam in the negative y-direction, calculated along the neutral axis of the model $(x, 0, 0)$, is given by the graphs in Figure 6. Note that in all of the graphs presented, the quantities t refer to the interface element thickness t_i. The six graphs are arranged so that the bending stiffness is constant in each graph. From the graphs, it can be seen that for any set of parameters containing $t_i = 0.01$ a significant change occurs in the y-displacement at the interface of the beam model. For $\mathcal{B} \geq 100$, the curves for $t_i = 0.1$ are quite close to the curves for $t_i = 1.0$. As expected, when the interface thickness is less than one, the bending stiffness becomes more sensitive to the value of the interface thickness ($\mathcal{B} = 12I/t_i^3$). However, it is desirable to have t_i as small as possible to prevent over-constraining the membrane behavior of the solid elements at the interface. Although the largest value for $\mathcal{B}$ used in the analysis was $100,000$, a larger value in combination with $t_i = 0.01$ might have produced better results.

The flexure stress σ_{xx} of the beam model is shown in Figure 7. The values of stress shown in the graphs of Figure 7 are obtained from the set of nodes defined by the line $(x, 0.5, 0)$ for the solid region and along the top surface of the shell region. For $t_i = 1.0$, the stress perturbation induced by the interface elements is attenuated within one element distance from the interface. For the other two values of t_i, the effect of the interface elements is transmitted through two element distances into the solid region and one element distance into the shell region. For $\mathcal{B} \geq 10,000$, the stress perturbations are attenuated within one element distance on either side of the interface.

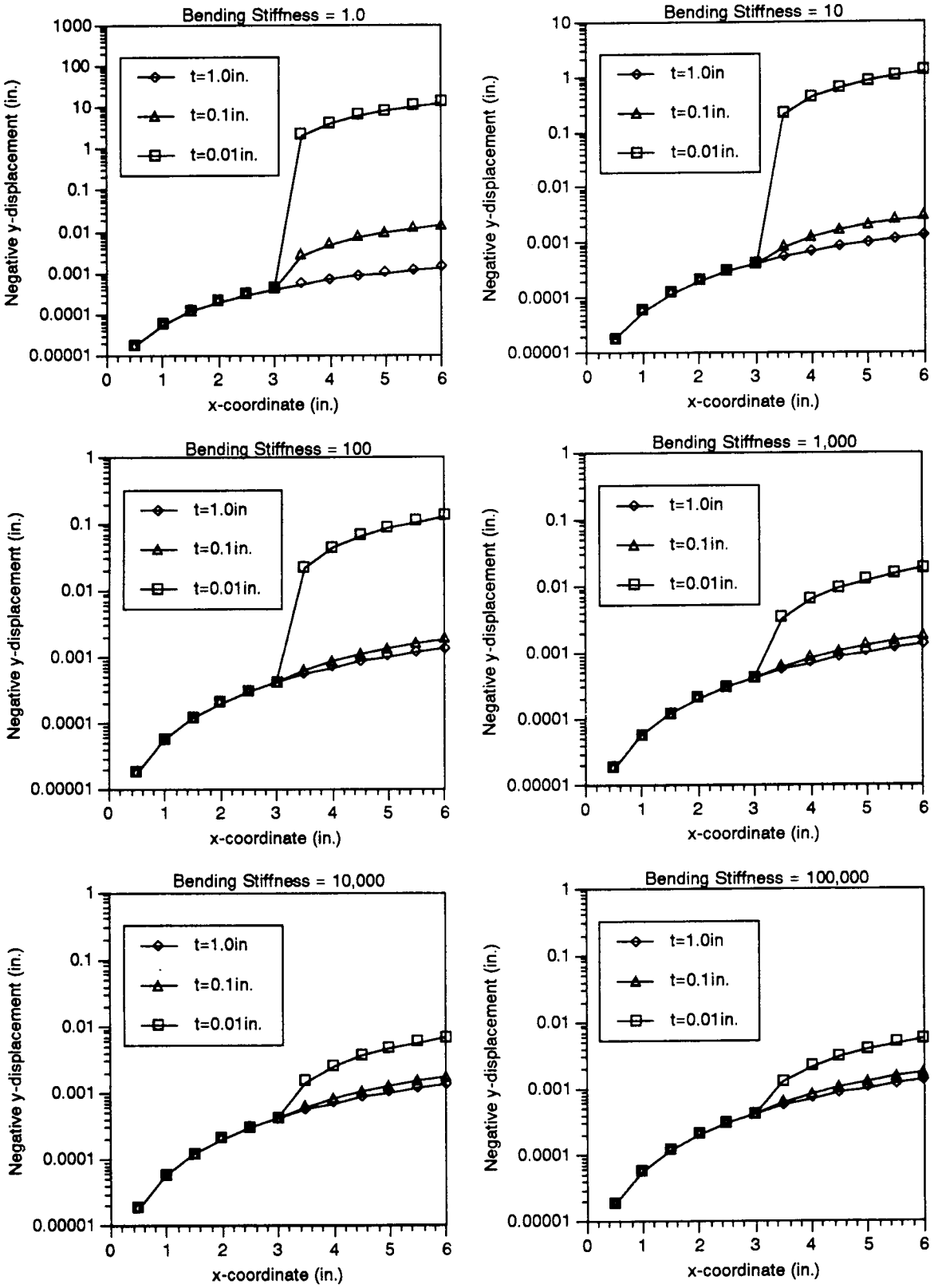

Figure 6: Vertical displacement of the neutral axis nodes of the first "beam" model (the cantilevered end is at $x = 0$).

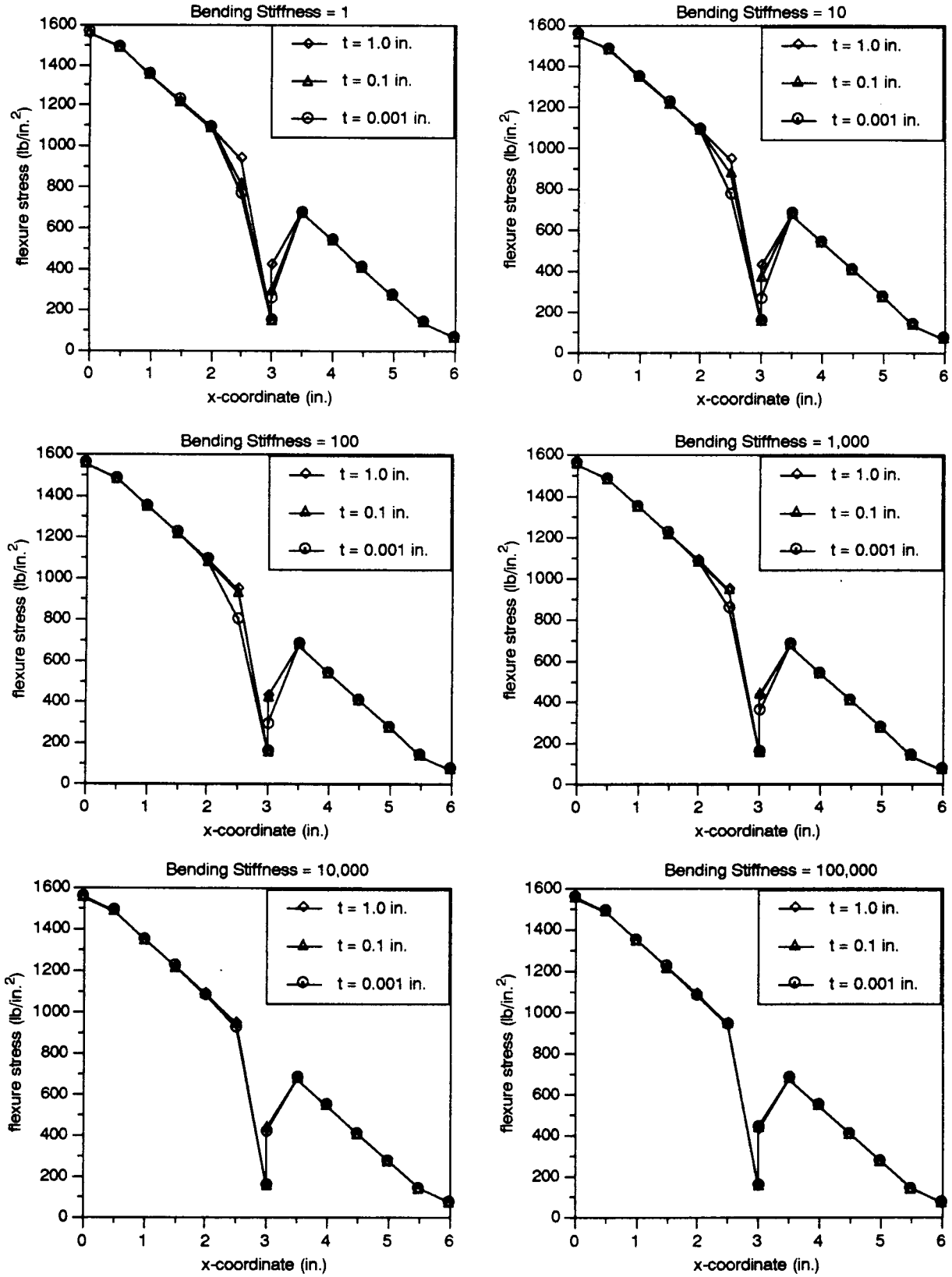

Figure 7: The flexure stress σ_{xx} of the nodes at $(x, 0.5, 0)$ for the beam model (along the top surface).

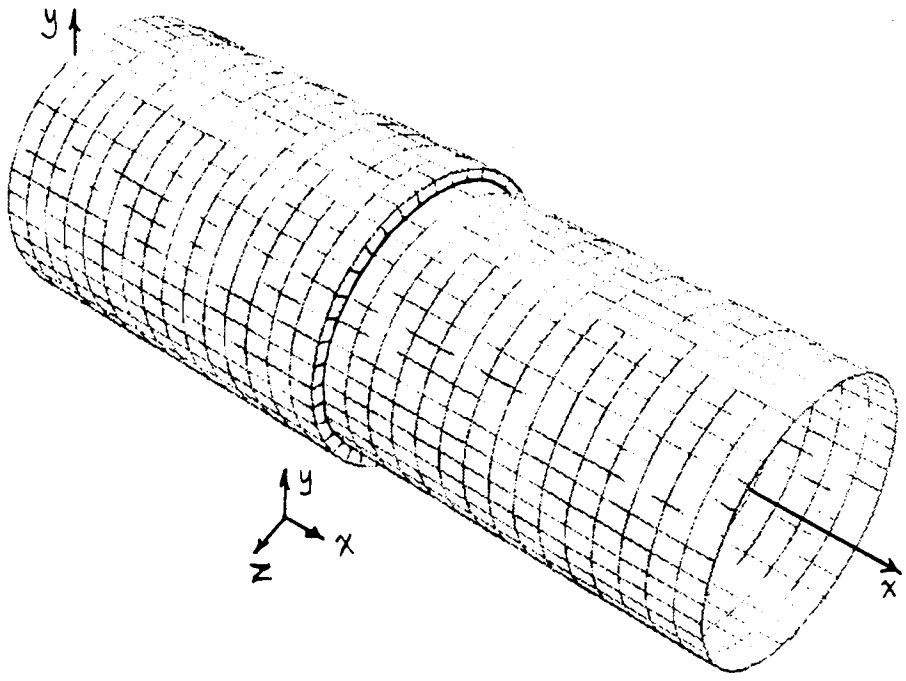

Figure 8: Case 2. The cantilevered tube model.

2.2 The Cantilevered Tube Problem

The finite element model used in this case consists of a cantilevered tube structure, having a middle-surface radius of 0.5 *in*. The solid region is modelled by two layers of CHEXA8 elements and the shell region is modelled by one layer of CQUAD4 elements. The finite element mesh is shown in Figure 8. The tube model has a total length of three inches, equally divided between solid and shell elements, and a thickness of 1/10 of an inch. A close-up view of the interface is shown in Figure 9. The tube model was loaded by an internal pressure of 50 *psi* in one load subcase and by a 10 *lb*. transverse load at the free end in the negative y-direction in the second subcase.

This case differs significantly from the cantilevered beam model. In this case, the sensitivity of the model to changes in the bending stiffness and interface thickness is not as great (for bending behavior). This is due in part to the geometry of the cross-section of the tube. On the sides of the tube, the bending behavior is transmitted more through translational *dof* than through rotational *dof* ("top" and "bottom" refer to locations on the tube model having coordinates where y is a maximum or a minimum; the "sides" of the tube have coordinates where y is near zero).

Analysis Results
The deformed geometry of the tube model under free end loading in the negative y-direction, and the resulting flexure stress σ_{xx} distribution, can be seen in Figure 10.

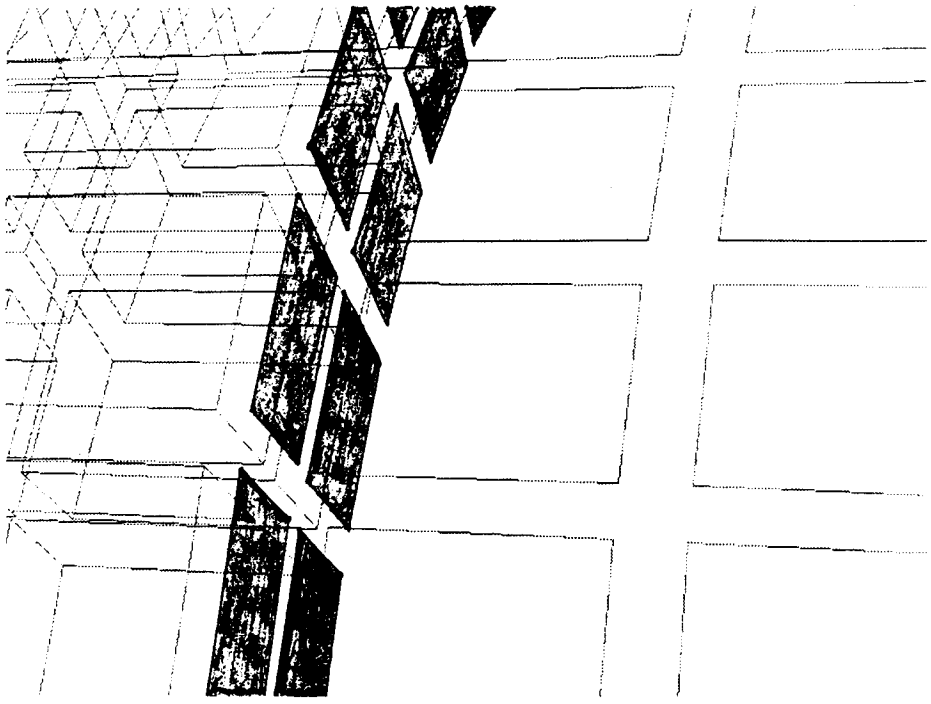

Figure 9: Case 2. Detail of the tube model solid/shell interface.

The sets of parameters associated with Figure 10 are $\{t_i = 1.0, \mathcal{B} = 1\}$. Figure 11 shows the deformed geometry of the tube model under pressure loading. Notice the over-constrained circumferential motion at the interface. In this particular example, where $t_i = 1.0$ and $\mathcal{B} = 1$, the membrane stiffness of the interface elements restricts normal circumferential deformation.

The y-displacements of the middle-surface nodes $(x, 0.5, 0)$ at the top of the model are shown in Figure 12. For all sets of parameters, the displacement distribution is smooth through the interface.

The flexure stress σ_{xx} of the middle-surface nodes at the top of the tube model is shown in Figure 13. The perturbations of σ_{xx} shown in the graphs do not appear to be sensitive to changes in $\mathcal{B}$. However, subcases having different values of t_i manifest different perturbations in σ_{xx}. The perturbations (for all subcases) are attenuated within three element distances from the interface into the solid elements and within one element distance into the shell elements. The σ_{xx} perturbations are similar in direction for $t_i = 1.0$ and $t_i = 0.1$, but are oppositely-directed in the subcases where $t_i = 0.01$.

Figure 14 contains graphs of the circumferential stress distribution along the middle-surface nodes on the top of the tube model due to internal pressure. It is obvious from Figure 14 that the interface thickness t_i greatly influences the behavior of the

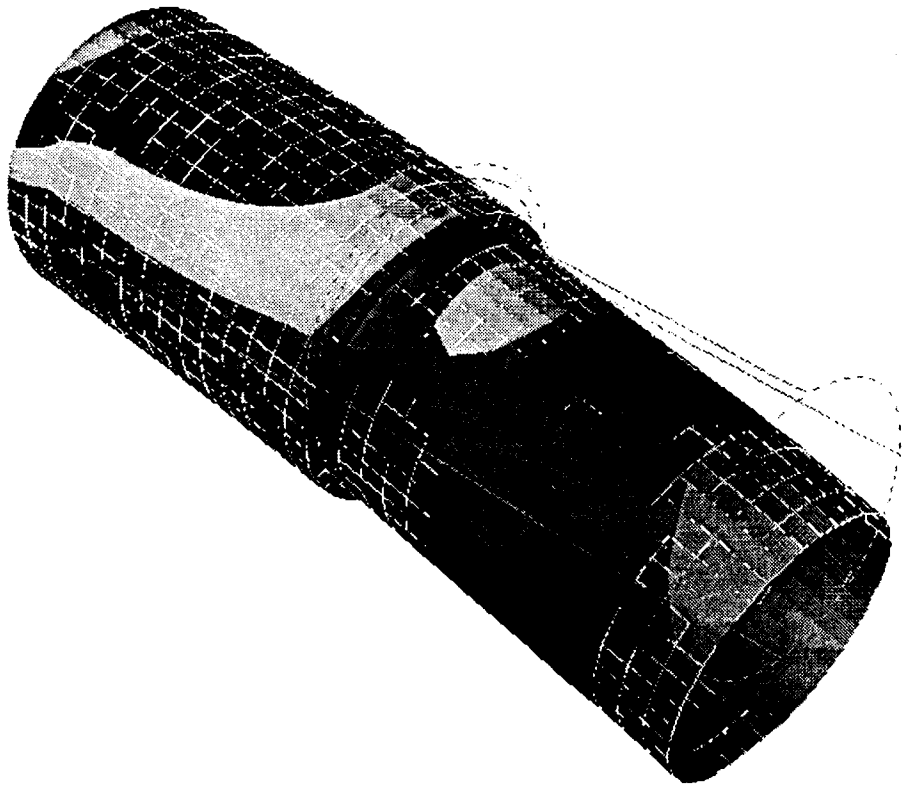

Figure 10: Deformed geometry of the tube model due to free end loading in the negative y-direction.

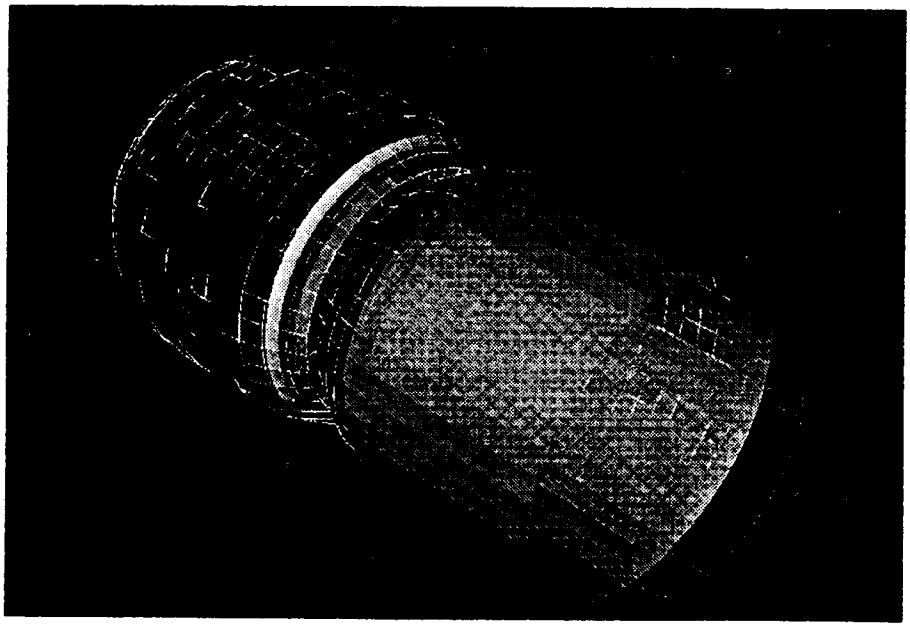

Figure 11: Deformed geometry of the tube model due to internal pressure. (Note the restricted circumferential deformation at the interface.)

tube model in the circumferential direction at the interface. Even for the subcases where $t_i = 0.01$, the membrane stiffness of the interface restricts the behavior of the tube interface. As one might expect, the bending stiffness has no discernible effect on the circumferential stresses $\sigma_{\theta\theta}$ shown in Figure 14. The $\sigma_{\theta\theta}$ perturbations due to the interface element membrane stiffness are transmitted through more elements than in the subcases where only the free-end load was applied.

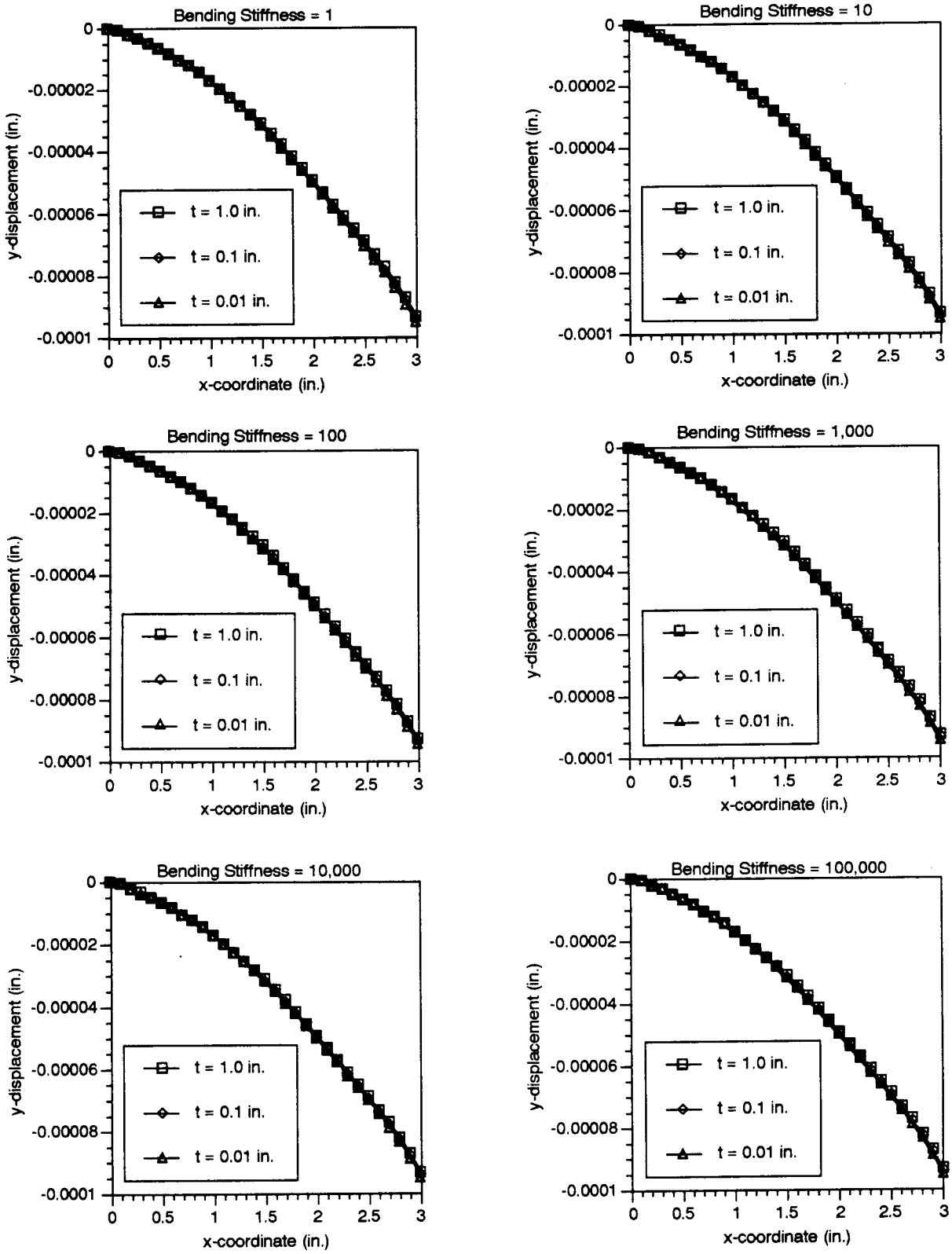

Figure 12: Vertical displacement of the middle-surface nodes along the coordinates $(x, 0.5, 0)$ (the cantilevered end is at $x = 0$).

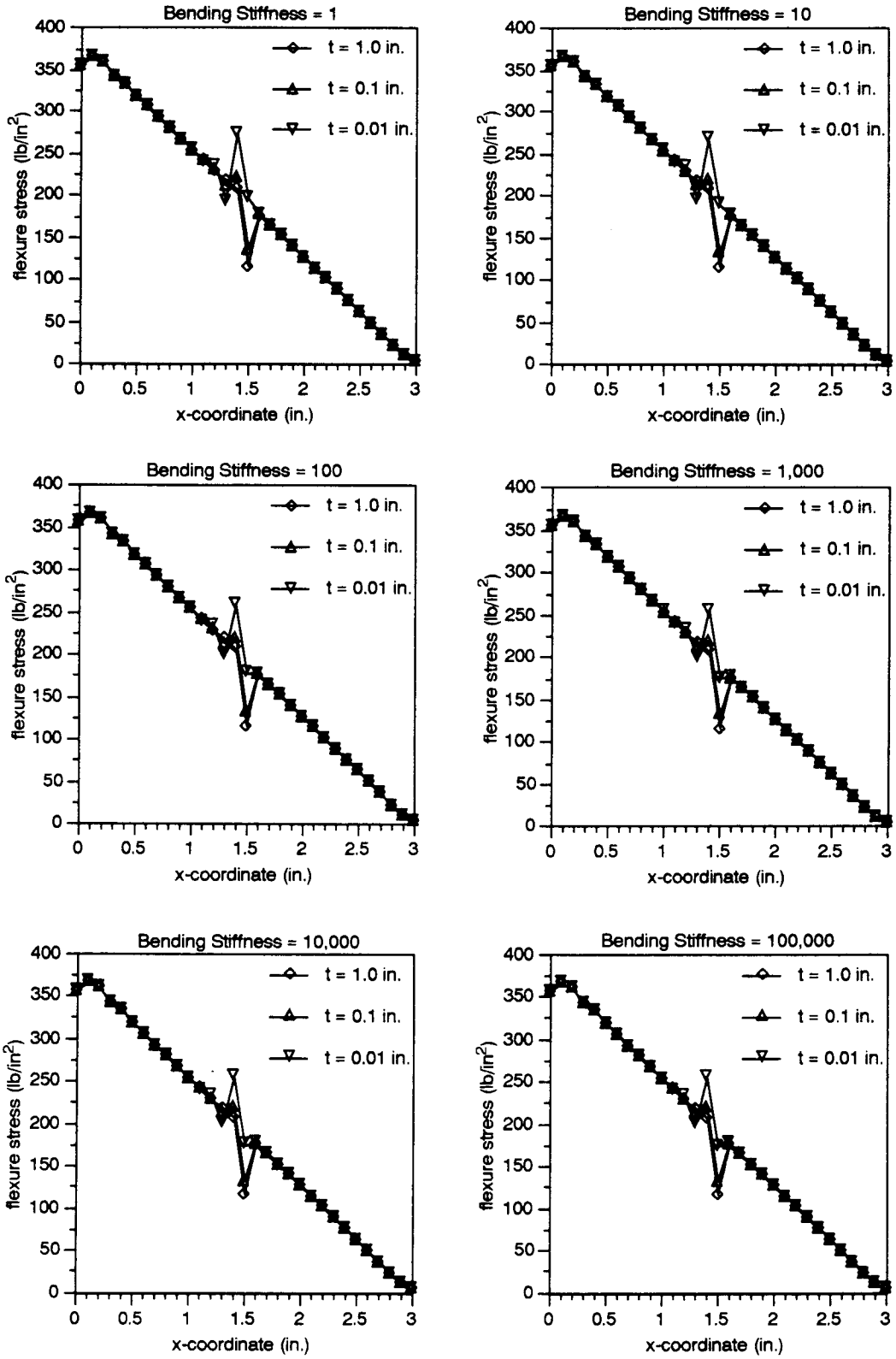

Figure 13: The flexure stress σ_{xx} of the nodes at $(x, 0.5, 0)$ (tube middle-surface surface).

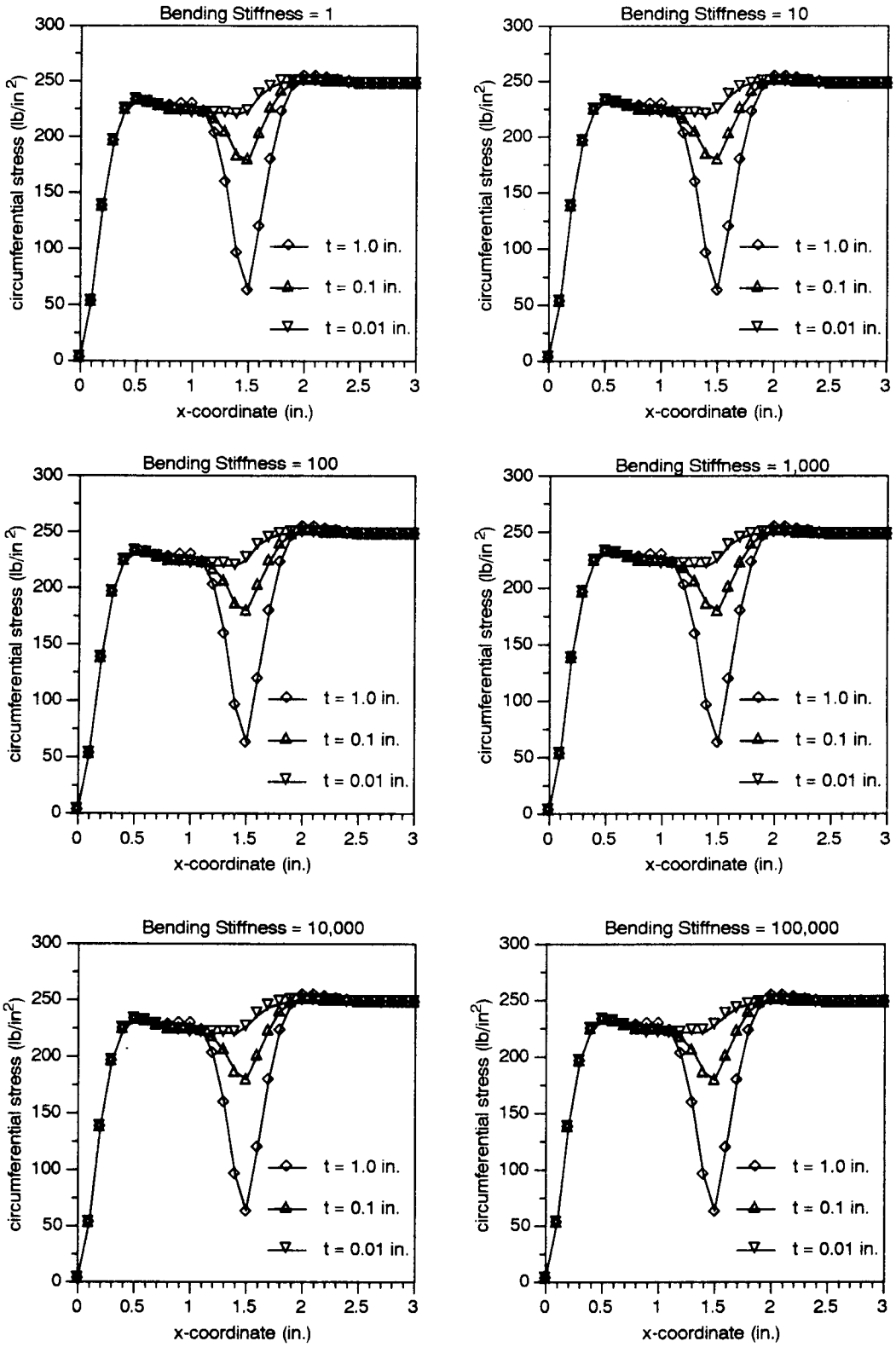

Figure 14: The circumferential stress $\sigma_{\theta\theta}$ of the nodes at $r = 0.5$ (the middle-surface surface).

3 Conclusion

Two examples utilizing the MSC/NASTRAN CQUAD4 element to interface solid and shell finite elements have been presented. In both examples, the thickness and the bending stiffness of the interface elements were varied to determine their effect on the behavior of the finite element model.

It was determined that the ideal set of interface element parameters would be the set having an extremely small thickness and an extremely large bending stiffness. This combination of parameters provides adequate transmission of forces/moments and displacements in bending. In addition, proper selection of the interface parameters ensures that the membrane stiffness of the interface elements does not adversely affect the behavior of the entire finite element model. Another factor in selecting the set of parameters to use in the interface element definition is the geometry of the finite element mesh at the interface. Although there is a rotational *dof* incompatibility at the interface when the CQUAD4 element is used, the CQUAD4 element appears to work rather well. The overly-constrained behavior induced by the CQUAD4 element at the interface damps out within a three element distance from the interface. Of course, ease of use in applying the CQUAD4 element at the interface, especially if done using a graphics pre/post-processor, is an important reason to use the CQUAD4 element.

In fact, only a bending stiffness is required to transmit the necessary *dof* at the interface. It should be noted that a better method of implementing the CQUAD4 element exists. Specifically, the analyst can choose only bending behavior for the interface elements by leaving the MID1 field blank in the PSHELL bulk data entry. The thickness value t_i can be specified in order to obtain the best combination with the bending stiffness $\mathcal{B}$ (≥ 1 is recommended). Although this paper does not include a study of the viability of this method, the author recommends it, as it is a more elegant way of implementing the CQUAD4 element at the interface between solid and shell elements.

Acknowledgement

The technical assistance and many helpful suggestions provided by Mr. Chuck Stack are greatly appreciated.

References

[1] Feld, Denis J., and Soudry, Jean G., "Modeling the Interface Between Shell and Solid Elements," *Proceedings of the MSC/NASTRAN World Users' Conference*, March 1983.

[2] MacNeal, Richard, "A Simple Quadrilateral Shell Element," *Computers & Structures*, Vol. 8, 1978, pp. 175–183.

[3] Schaeffer, Harry G., *MSC/NASTRAN Primer*, Shaeffer Analysis, Inc., Mont Vernon, New Hampshire, 1979.

[4] *MSC/NASTRAN User's Manual*, Version 66A, The MacNeal-Schwendler Corporation, Los Angeles, CA, November 1988.